Hindawi Publishing Corporation
Journal of Spectroscopy
Volume 2015, Article ID 730753, 7 pages
http://dx.doi.org/10.1155/2015/730753

Research Article

Investigation on Structural and Optical Properties of Willemite Doped Mn^{2+} Based Glass-Ceramics Prepared by Conventional Solid-State Method

Nur Farhana Samsudin,[1] Khamirul Amin Matori,[1,2] Josephine Ying Chi Liew,[2] Yap Wing Fen,[1,2] Mohd Hafiz Mohd Zaid,[2] and Zarifah Nadakkavil Alassan[2]

[1]*Materials Synthesis and Characterization Laboratory, Institute of Advanced Technology, Universiti Putra Malaysia (UPM), 43400 Serdang, Selangor, Malaysia*
[2]*Department of Physics, Faculty of Science, Universiti Putra Malaysia (UPM), 43400 Serdang, Selangor, Malaysia*

Correspondence should be addressed to Khamirul Amin Matori; khamirul@upm.edu.my

Received 3 July 2015; Revised 3 November 2015; Accepted 9 November 2015

Academic Editor: Javier Garcia-Guinea

Mn-doped willemite (Zn_2SiO_4:Mn^{2+}) glass-ceramics derived from ZnO-SLS glass system were prepared by a conventional melt-quenching technique followed by a controlled crystallization step employing the heat treatment process. Soda lime silica (SLS) glass waste, ZnO, and MnO were used as sources of silicon, zinc, and manganese, respectively. The obtained glass-ceramic samples were characterized using the X-ray diffraction (XRD), Field Emission Scanning Electron Microscopy (FESEM), Fourier Transform Infrared (FTIR), UV-Visible (UV-Vis), and photoluminescence (PL) spectroscopy. The results of XRD revealed that ZnO crystal and willemite (β-Zn_2SiO_4) were presented as major embedded crystalline phases. This observation was consistent with the result of FESEM which showed the presence of irregularity in shape and size of willemite crystallites. FTIR spectroscopy exhibits the structural evolution of willemite based glass-ceramics. The optical band gap shows a decreasing trend as the Mn-doping content increased. Photoluminescent technique was applied to characterize the role of Mn^{2+} ions when entering the willemite glass-ceramic structure. By measuring the excitation and emission spectra, the main emission peak of the glass-ceramic samples located at a wavelength of 585 nm after subjecting to 260 nm excitations. The following results indicate that the obtained glass-ceramics can be applied as phosphor materials.

1. Introduction

Recently, phosphor materials have become the key component of optoelectronic technological development. Many devices are basically composed of lighting units made with light emitting diode (LED) which is built up from one or more phosphor materials [1]. The basic principle of those phosphors is associated with the luminescence properties of the transition metal or rare earth ions doped in the selected host materials. Thus, type of the transition metal and rare earth ions and characteristic of the host materials are the main consideration during phosphor material development [2–5]. Among the transition metal ions, manganese (Mn^{2+}) is recognized as an efficient wide range of emission colors luminescent phosphors due to the transition of the $3d^5$ electrons from the $^4T_1(^4G)$ excited-state to the $^6A_1(^6S)$ ground-state which are used in Cathode Ray Tubes (CRT), Plasma Displays Panels (PDPs), and also fluorescent lamps [6–10].

The host materials have been obtained conventionally in two common forms, single crystal or ceramic powder, with varieties of crystal structures. For LED application, the host materials are required to show excellence in mechanical, optical, and thermal properties [11]. These requirements have brought glass-ceramics materials as the best candidate for the development of a new generation of LED. Glass-ceramics such as willemite (Zn_2SiO_4) exhibit good mechanical strength, high luminescence efficiency, high color purity, strong chemical durability, and highly thermal stabilities and these properties are suitable for LED applications [12–14].

Willemite exists in three different phases which are α-, β-, and γ-Zn_2SiO_4 and shows different colors of emission: green emission (α-Zn_2SiO_4), yellow emission (β-Zn_2SiO_4), and red color (γ-Zn_2SiO_4) [15]. The most common practical crystalline phase, α-Zn_2SiO_4 phase, is usually being used in many displays and light emitting devices due to its behavior of strong green emission under ultraviolet light or an electron beam.

Commercially, inorganic phosphors including Zn_2SiO_4:Mn^{2+} have been prepared using conventional solid-state method [16]. The reaction will be carried out at temperature ranges from 1100°C to 1400°C for 2 to 4 hours with ZnO, SiO_2, and MnO or $MnCO_3$ as starting materials and provide irregularly shaped particles. As solid-state reaction is a well-established method for synthesizing many phosphors including α-Zn_2SiO_4:Mn^{2+}, the crystalline phase of phosphor is commonly produced via solid diffusion among solid starting materials at temperatures higher than 1000°C and for processing times of several hours [17]. Recently, many new methods to prepare Zn_2SiO_4:Mn^{2+} green phosphors were proposed and extensively studied in order to improve the material properties and also enhance their performance by reducing the time and processing temperature [18]. However, the materials produced are difficult to commercialize due to complexity of the preparation and high cost of the materials used. Solid-state method offers several advantages compared to other methods such as production in a large scale which is less complex and low in production cost.

The present study is attempted to prepare the willemite glass-ceramic derived from the ZnO-SLS glass system with MnO doping. Then, our report and discussion will focus on the structural, phase formation, microstructure, and optical properties of the glass-ceramics. The obtained information will be used for further serial works of an effort to develop the glass-ceramic phosphor proposed for a new generation of LED and related applications.

2. Experimental Details

The parent glass sample of the Mn^{2+} doped ZnO-SLS system was prepared from a 30 g batch with the reagent grade chemicals, that is, ZnO (99.99% Aldrich), MnO (99.9% Aldrich), and SLS waste glass, using conventional melt-quenching method. All starting materials were exactly weighed due to the chemical formula of $((ZnO)_{0.5}(SLS)_{0.5})_{1-y}(MnO)_y$, where $y = 0$, 0.01, 0.02, 0.03, and 0.10, and mixed in a ceramic milling jar for several hours to ensure homogeneous mixing. The detailed compositions of the samples are given in Table 1. Then, the glass batches were melted in an alumina crucible at 1400°C for 2 hours. The melts were quenched in the container containing cold water to obtain the transparent glass frits. The glass frits were dried under sunlight for 24 hours and then milled in a high-speed porcelain mill for 24 hours, resulting in powders with a mean particle size of 45 μm. Next, the mixed powders were uniaxially pressed into pellets of 13 mm in diameter and 2 mm in thickness with an applied load of 5 tons for 10 min using polyvinyl alcohol (PVA) as the binders. After that, the selected pellet samples were then subjected to the heat treatment process at 600°C with duration of 2 hours in the electrical furnace and under atmosphere of normal air and then ready for further characterization. After the heat treatment process, the pellet samples are grained to obtain the specific size powder for the further analysis.

Table 1: Chemical compositions of $(SLS_{0.5}\ ZnO_{0.5})_y(MnO)_{1-y}$ glass precursor.

Sample	SLS (g)	ZnO (g)	MnO (g)	Sample powder (g)
Undoped	30.00	30.00	0.00	60.00
1 wt.%	29.70	29.70	0.60	60.00
2 wt.%	29.40	29.40	1.20	60.00
3 wt.%	29.10	29.10	1.80	60.00
10 wt.%	27.00	27.00	6.00	60.00

In this research, the chemical composition of SLS-ZnO doped MnO glass precursor was characterized using EDX-720/800HS/900HS. The X-ray diffraction (PANalytical (Philips) X'Pert Pro PW 3050/60 CuKα radiation) was used to confirm the amorphous state of the parent glass sample and to identify the crystalline phase formed in the glass-ceramics samples. The X-ray beam diffracted on the samples through an angle range of $2\theta = 20^\circ$–80° using 0.02° steps. Field Emission Scanning Electron Microscopy (FESEM, FEI Nova NanoSEM 30) was employed for the microstructural observation on the top surface and cross section area of the glass-ceramic samples surfaces. Chemical bonding existing in the samples was characterized using Fourier Transform Infrared Spectroscopy (FTIR, Perkin Elmer (US) Spectrum 100 spectrometer with Universal Attenuated Total Reflectance (ATR)). The infrared spectra were recorded in the range of wavenumber of 400 cm^{-1}–4000 cm^{-1} with a resolution of 4 cm^{-1}. UV-Visible (UV-Vis, Shimadzu UV-Vis-NIR) spectroscopy is used in this research to gain the absorbance spectra of the glass-ceramic samples. The optical band gap energy is given by [19]

$$\alpha h\nu = C\left(h\nu - E_g\right), \tag{1}$$

where α is the optical absorption coefficient, C is the constant independent of photon energy ($h\nu$), and E_g is the direct allowed optical band gap energy. The excitation and emission spectra were measured by PL, Perkin-Elmer LS 55 Fluorescence spectrometer with a 450 W xenon lamp at room temperature.

3. Results and Discussion

The chemical composition obtained was given in Table 2. Eight oxide elements and small percentage of unknown oxide were detected in the glass precursor samples. Elements like SiO_2, CaO, Na_2O, Al_2O_3, K_2O, and MgO are originated from SLS waste. From Table 2, the increases in MnO addition have resulted in a reduction to other elements in glass samples.

Figure 1 shows the XRD powder patterns of the undoped and Mn-doped willemite based glass-ceramic samples that have been sintered at 600°C for 2 hours. In Figure 1, all the diffraction peaks are in good agreement with those of the standard pattern reported by the Joint Committee on Powder

Table 2: Analysis of chemical composition of SLS-ZnO doped MnO glass precursor using EDXRF.

Elements	SiO_2	CaO	Na_2O	Al_2O_3	K_2O	MgO	ZnO	MnO	Others
Undoped	34.60	5.55	6.35	1.50	0.90	1.10	49.80	0.00	0.20
1 wt.%	34.20	5.60	6.10	1.00	0.80	1.10	50.22	0.88	0.10
2 wt.%	35.10	5.30	6.20	1.20	0.80	1.00	48.35	1.85	0.20
3 wt.%	35.20	5.20	6.00	1.40	0.90	0.90	47.41	2.79	0.20
10 wt.%	33.40	5.10	4.90	1.30	0.80	1.00	43.21	9.83	0.45

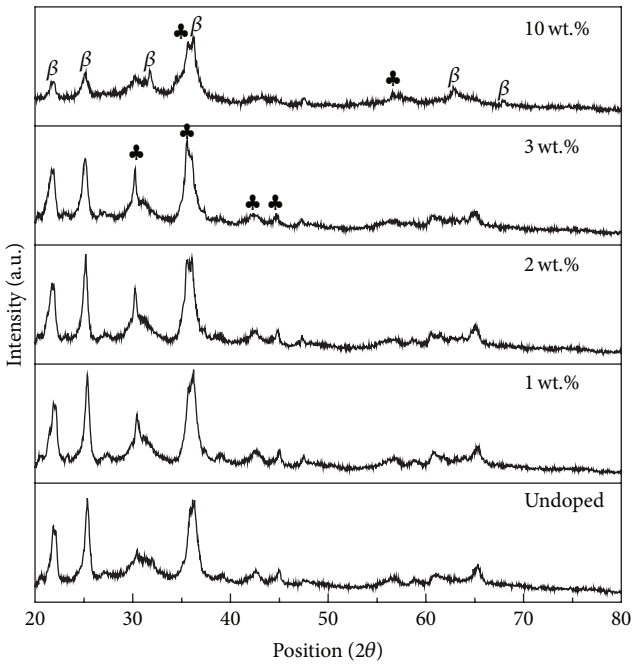

Figure 1: XRD pattern of undoped and Mn-doped Zn_2SiO_4 based glass-ceramic sintered at 600°C.

Diffraction Standard (JCPDS number 14-0653), indicating that the prepared samples are orthorhombic β-Zn_2SiO_4 with lattice parameter of $a = 8.40$ Å, $b = 5.10$ Å, and $c = 32.20$ Å and $\alpha = 90.00^\circ$, $\beta = 90.00^\circ$, and $\gamma = 90.00^\circ$. All the glass-ceramics samples that have been sintered at 600°C exhibit six major diffraction peaks at 29 = 21.82°, 25.06°, 31.24°, 36.19°, 60.89°, and 65.18° corresponding to (2 0 2), (0 0 9), (2 1 5), (0 2 3), (0 2 17), and (3 3 4) planes [20]. Among polymorphic willemite, the β-phase is known as the metastable phases and can only occur under a certain condition. An additional peak in XRD pattern exist from the possible base precursor such as crystalline ZnO was found at the pattern [21, 22]. The residual peaks agree well with the standard pattern of ZnO (JCPDS number 36-1451). The intensity of the diffraction peaks increased from undoped to the 3 wt.% of Mn-doped and decreased when the higher doping concentration was introduced which indicates a loss of crystallinity due to lattice distortion. Mn^{2+} ions are incorporated into the periodic crystal lattice; a strain is induced into the system, resulting in the alteration of the lattice periodicity and decrease in crystal symmetry [23].

FESEM analysis was performed to study the size, shape, and morphology of glass-ceramics. Figures 2(a)–2(e) show the morphology of the undoped and Mn-doped willemite based glass-ceramics samples sintered at 600°C prepared at different weight percentage of Mn-doping. FESEM observation showed an aggregation and irregularity in shape and size [24–26]. The micrographs reveal that there are tiny crystals growing on the surface of the samples as an indication of formation of ceramic. Thus, these results agree well with the XRD results since the nature of the samples is crystalline with willemite and ZnO phase detected. The micrographs show that the particle sizes vary from 2 μm to 10 μm. The dependency of the photoluminescence of the phosphors on shape and size of the phosphors is generally acknowledged. Thus, the particle size and shape of the sample need to be controlled in order to achieve maximum quantum efficiency through energy absorption. Other researchers who also prepared Zn_2SiO_4:Mn^{2+} using solid-state method reported that their particles were composed of rectangular shaped grains with relatively large size of 1-2 pm [9].

The FTIR spectra of willemite doped with manganese sintered at 600°C were measured in the wavenumber range of 400 to 4000 cm^{-1} as shown in Figure 3. The infrared spectra are used to get more information about the presence of different structural groups in the material. These FTIR spectra were analyzed and compared with the previous literature and summarized in Table 3. In all samples, the characteristics bending mode of Si-O-Si bond is formed around 450 cm^{-1}. Efimov reported that Si-O-Si bending modes are exhibited at position lower than 500 cm^{-1}, which fitted in 460 cm^{-1} [27]. Bands around 570 cm^{-1} are observed in all samples, which can be attributed to the symmetric stretching vibrational mode of ZnO_4. The characteristics of symmetric stretching vibrational mode of Zn-O-Si and asymmetric stretching vibrational mode of SiO_4 are observed at around 690 cm^{-1} and 890 cm^{-1}, respectively [28]. The whole spectrum of each glass-ceramics sample seems to be repetitive pattern compared to that of undoped willemite except for the intensity of all the bands for willemite that have been doped with 10 wt.% of Mn. At 10 wt.% Mn-doping concentration, the intensity of the spectra appeared to be less intense compared to the lower dopant concentration. The appearance of both SiO_4 and ZnO_4 groups clearly suggests the formation of willemite phase which is in good agreement with the XRD result as it detected the formation of willemite and ZnO phase.

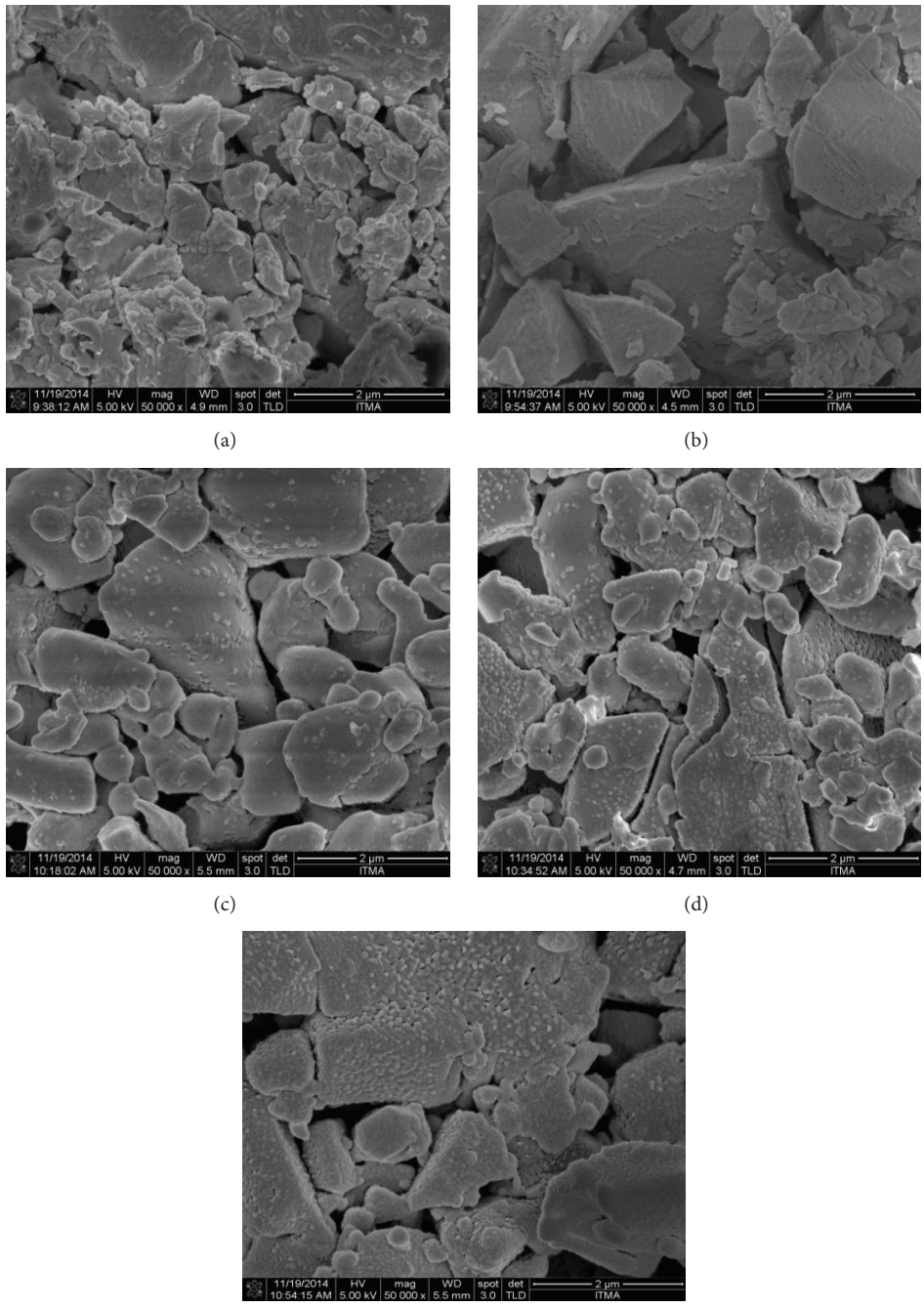

Figure 2: FESEM micrograph of undoped and Mn-doped Zn_2SiO_4 based glass-ceramic sintered at 600°C: (a) undoped, (b) 1 wt.% MnO, (c) 2 wt.% MnO, (d) 3 wt.% MnO, and (e) 10 wt.% MnO.

Absorption spectra of undoped and Mn-doped willemite based glass-ceramic samples recorded in the region of 250–800 nm are demonstrated in Figure 4. From the absorption curve, it clearly can be seen that the intensive absorption occurs in the range of 250–390 nm. In this study, the fundamental absorption edge of the samples is assumed to be the direct transition [29]. From the plot of $(\alpha hv)^2$ against hv, the value of optical band gap energy, E_g, is obtained by extrapolating the linear fitted regions to $(\alpha hv)^2 = 0$. The plot of $(\alpha hv)^2$ against (hv) shows a linear dependence. The band gap energy (E_{opt}) is determined by extrapolating the linear part of the spectrum $(\alpha hv)^2$ curve towards the (hv) axis in Figure 5.

The obtained E_{opt} values are compiled in Table 4. It is observed that the optical band gap of the samples as shown in Table 4 decreased as the percentage of doping content

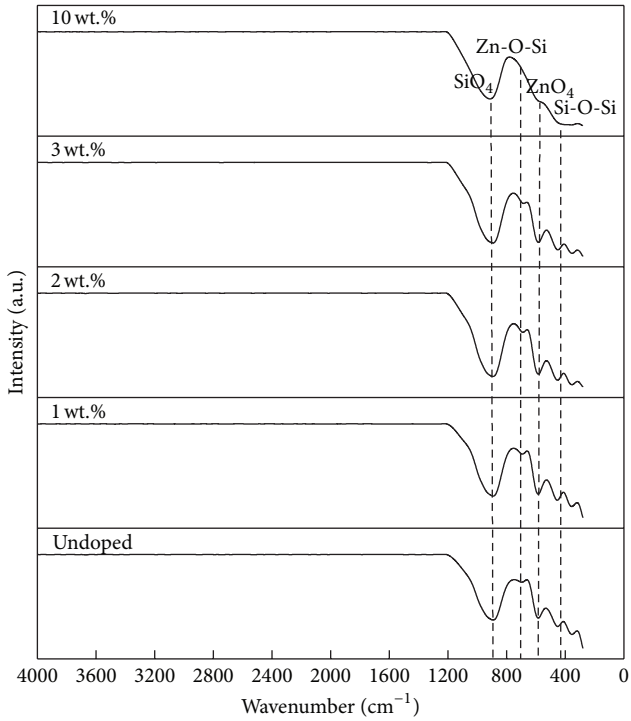

Figure 3: FTIR pattern of undoped and Mn-doped Zn_2SiO_4 based glass-ceramic sintered at 600°C.

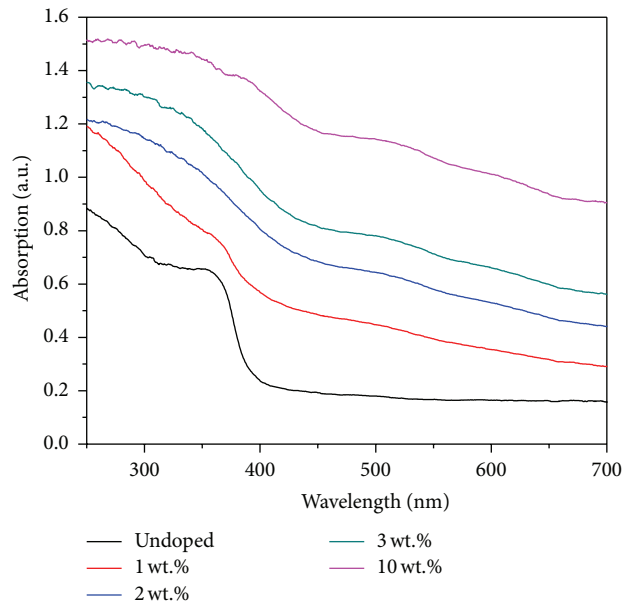

Figure 4: Absorption spectra of undoped and Mn-doped Zn_2SiO_4 based glass-ceramic sintered at 600°C.

increased. Omri et al. explained that the decrease in optical band gap after the Mn incorporation is due to the Mn defects in the bands [30]. These Mn^{2+} defects will result in the absorption of incident photons. Thus, the band gap is affected due to the strong internal forces. The electrons that

Table 3: FTIR spectral bands assigned to the vibrational modes.

Wavenumbers (cm^{-1})	Assignment of vibrational mode
~450	Si-O-Si bending mode
~570	ZnO_4 symmetric stretching vibrational mode
~690	Zn-O-Si symmetric stretching vibrational mode
~890	SiO_4 asymmetric stretching vibrational mode

Table 4: Band gap energy for undoped and Mn-doped Zn_2SiO_4 sintered at 600°C.

Percentage of MnO (wt.%)	Energy of gap (eV)
Undoped	3.96
1 wt.%	3.73
2 wt.%	3.19
3 wt.%	2.99
10 wt.%	2.58

are responsible for the transition from the valence band to the conduction band however need greater energy to jump.

Figure 6 shows the PL emission spectra peaking at 585 nm for different Mn percentage at an excitation at 260 nm. The emission intensity of the phosphors prepared by conventional solid-state methods also was found to be at 585 nm after firing at 700–750°C [31]. In this research, the samples prepared show increase in emission intensity as the percentage of the Mn-doping increased up to 3 wt.% and however decreased at the high doping content of 10 wt.%. The maximum emission intensity can be observed at 3 wt.% of doping content. Tsai et al. reported that the intensity of the emission spectra increased with increasing in Mn content up to 6% and however decreased significantly as the doping increased above 8% [32]. This trend has been attributed to the concentration quenching phenomenon since, at low concentration of dopant ions, the concentration quenching effects are said to be negligible due to relatively large average distance between Mn^{2+} ions [33]. This emission wavelength is attributed to the yellow emission. As being confirmed by earlier literature, the yellow emission of β-Zn_2SiO_4 comes from the same sources with α-Zn_2SiO_4 which is the transition from $^4T_1(^4G) \rightarrow {}^6A_1(^6S)$ of the doping Mn^{2+} ions substituted in Zn^{2+} sites of the Zn_2SiO_4 lattice. Thus, the oxidation state for the Mn ions in Zn_2SiO_4:Mn is +2 and 4− for the oxygen atoms which is also the same as the oxidation state for Zn ions.

4. Conclusion

In summary, undoped and Mn-doped willemite (Zn_2SiO_4:Mn^{2+}) based glass-ceramic from ZnO-SLS system have been prepared using melt-quench method. Zn_2SiO_4:Mn^{2+} glass-ceramics were obtained after sintering process at 600°C for 2 hours. The structural and optical properties of these glass-ceramics have been studied in detail. The structural characterization verifies the crystalline phases of glass-ceramic

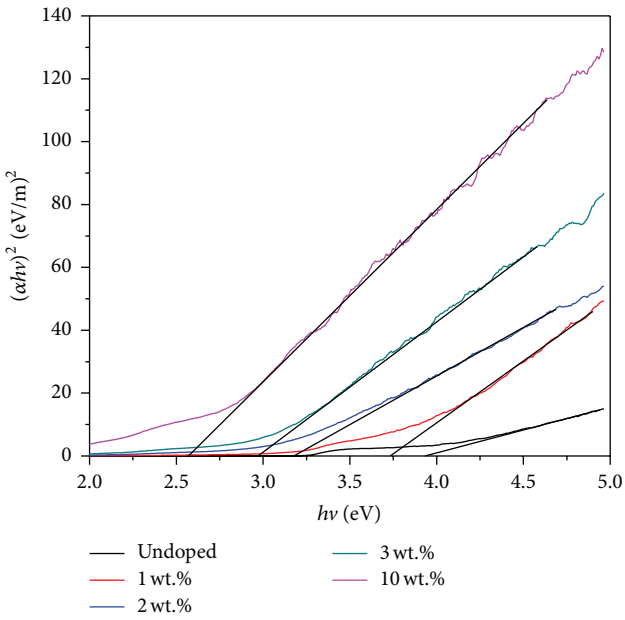

FIGURE 5: Plot of $(\alpha hv)^2$ versus photon energy (hv).

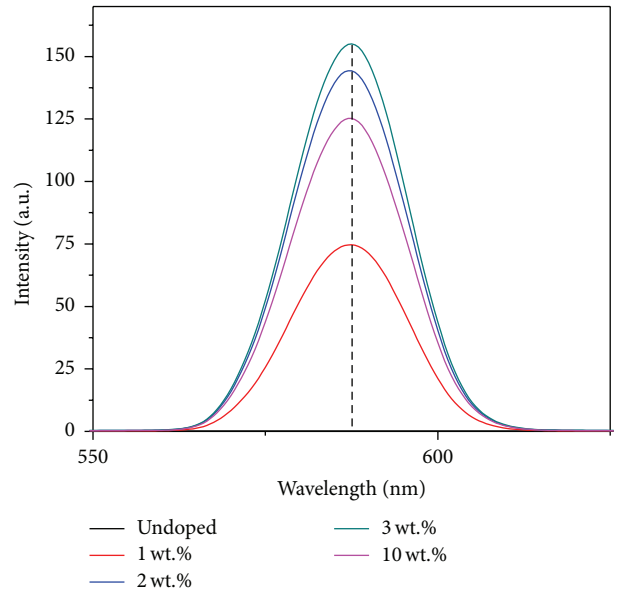

FIGURE 6: Emission spectra of undoped and Mn-doped Zn_2SiO_4 based glass-ceramic sintered at 600°C ($\lambda_{excitation}$ = 260 nm, $\lambda_{emission}$ = 585 nm). Lines are drawn to guide the eye.

and formation of β-Zn_2SiO_4, ZnO, and SiO_2 crystal. Investigations of optical band gap show that E_g decreased from 3.962 eV to 2.573 eV as we move towards higher concentration of MnO. The emission wavelength was obtained at 585 nm which is attributed to yellow emission. The emission intensity amplified as the dopant concentration increased to 3 wt.% and decreased at 10 wt.% of dopant concentration due to the concentration quenching phenomenon.

Conflict of Interests

The authors declare that there is no conflict of interests regarding the publication of this paper.

Acknowledgments

The researchers gratefully acknowledge the financial support for this study from the Malaysian Ministry of Higher Education (MOHE) and Universiti Putra Malaysia through the Fundamental Research Grant Scheme (FRGS) and *Inisiatif Putra Berkumpulan* (IPB) research grant.

References

[1] J. Jeong, M. Jayasimhadri, H. S. Lee et al., "Photoluminescence and phosphorescence properties of image phosphor for UV-based white-LEDs," *Physica B: Condensed Matter*, vol. 404, pp. 2016–2019, 2009.

[2] I. W. Lenggoro, F. Iskandar, H. Mizushima, B. Xia, K. Okuyama, and N. Kijima, "One-step synthesis for Zn_2SiO_4:Mn particles 0.3–1.3 μm in size with spherical morphology and non-aggregation," *Japanese Journal of Applied Physics*, vol. 39, no. 10, pp. L1051–L1053, 2000.

[3] H. Cui, M. Zayat, and D. Levy, "Nanoparticle synthesis of willemite doped with cobalt ions ($Co_{0.05}Zn_{1.95}SiO_4$) by an epoxide-assisted sol-gel method," *Chemistry of Materials*, vol. 17, no. 22, pp. 5562–5566, 2005.

[4] Y. Mao, J. Y. Huang, R. Ostroumov, K. L. Wang, and J. P. Chang, "Synthesis and luminescence properties of Erbium-doped Y_2O_3 nanotubes," *The Journal of Physical Chemistry C*, vol. 112, no. 7, pp. 2278–2285, 2008.

[5] K.-S. Sohn, B. Cho, H. D. Park, Y. G. Choi, and K. H. Kim, "Effect of heat treatment on photoluminescence behavior of Zn_2SiO_4:Mn phosphors," *Journal of the European Ceramic Society*, vol. 20, no. 8, pp. 1043–1051, 2000.

[6] K.-S. Sohn, B. Cho, and H. D. Park, "Photoluminescence behavior of manganese-doped zinc silicate phosphors," *Journal of the American Ceramic Society*, vol. 82, no. 10, pp. 2779–2784, 1999.

[7] M. Tanaka, "Photoluminescence properties of Mn^{2+}-doped II-VI semiconductor nanocrystals," *Journal of Luminescence*, vol. 100, no. 1–4, pp. 163–173, 2002.

[8] A. Patra, G. A. Baker, and S. N. Baker, "Effects of dopant concentration and annealing temperature on the phosphorescence from Zn_2SiO_4:Mn^{2+} nanocrystals," *Journal of Luminescence*, vol. 111, no. 1-2, pp. 105–111, 2005.

[9] T. H. Cho and H. J. Chang, "Preparation and characterizations of Zn_2SiO_4:Mn green phosphors," *Ceramics International*, vol. 29, no. 6, pp. 611–618, 2003.

[10] J. El Ghoul, C. Barthou, M. Saadoun, and L. El Mir, "Synthesis and optical characterization of SiO_2/Zn_2SiO_4:Mn nanocomposite," *Physica B*, vol. 405, no. 2, pp. 597–601, 2010.

[11] M. Kang and S. Kang, "Effects of Al_2O_3 addition on physical properties of diopside based glass-ceramics for LED packages," *Ceramics International*, vol. 38, supplement 1, pp. S551–S555, 2012.

[12] C. Feldmann, T. Jüstel, C. R. Ronda, and P. J. Schmidt, "Inorganic luminescent materials: 100 years of research and application," *Advanced Functional Materials*, vol. 13, no. 7, pp. 511–516, 2003.

[13] S. Zhang, "Vacuum-ultraviolet/visible conversion phosphors for plasma display panels," *IEEE Transactions on Plasma Science*, vol. 34, no. 2, pp. 294–304, 2006.

[14] H. Liang, Q. Zeng, Z. Tian et al., "Intense emission of $Ca_5(PO_4)_3F:Tb^{3+}$ under VUV excitation and its potential application in PDPs," *Journal of the Electrochemical Society*, vol. 154, no. 6, pp. J177–J180, 2007.

[15] M.-T. Tsai, Y.-H. Lin, and J.-R. Yang, "Characterization of manganese-doped willemite green phosphor gel powders," *IOP Conference Series: Materials Science and Engineering*, vol. 18, no. 3, Article ID 032026, 5 pages, 2011.

[16] W. M. Yen and M. J. Weber, *Inorganic Phosphors*, CRC Press, Boca Raton, Fla, USA, 2004.

[17] C. Barthou, J. Benoit, P. Benalloul, and A. Morell, "Mn^{2+} concentration effect on the optical properties of Zn_2SiO_4:Mn phosphors," *Journal of the Electrochemical Society*, vol. 141, no. 2, pp. 524–528, 1994.

[18] M. Takesue, H. Hayashi, and R. L. Smith Jr., "Thermal and chemical methods for producing zinc silicate (willemite): a review," *Progress in Crystal Growth and Characterization of Materials*, vol. 55, no. 3-4, pp. 98–124, 2009.

[19] R. A. Smith, *Semiconductors*, Cambridge University Press, Cambridge, UK, 1978.

[20] Y. Jiang, J. Chen, Z. Xie, and L. Zheng, "Syntheses and optical properties of α- and β-Zn_2SiO_4:Mn nanoparticles by solvothermal method in ethylene glycol-water system," *Materials Chemistry and Physics*, vol. 120, no. 2-3, pp. 313–318, 2010.

[21] A. Patra, G. A. Baker, and S. N. Baker, "Synthesis and luminescence study of Eu^{3+} in Zn_2SiO_4 nanocrystals," *Optical Materials*, vol. 27, no. 1, pp. 15–20, 2004.

[22] C. B. Babu and S. Buddhudu, "Emission spectra of Tb^{3+}: Zn_2SiO_4 and Eu^{3+}: Zn_2SiO_4 sol-gel powder phosphors," *Journal of Spectroscopy Dynamics*, vol. 4, pp. 1–8, 2013.

[23] M. Pal, U. Pal, J. M. G. Y. Jiménez, and F. Pérez-Rodríguez, "Effects of crystallization and dopant concentration on the emission behavior of TiO_2:Eu nanophosphors," *Nanoscale Research Letters*, vol. 7, article 1, 12 pages, 2012.

[24] A. M. Hu, M. Li, D. L. M. Dali, and K. M. Liang, "Crystallization and properties of a spodumene-willemite glass ceramic," *Thermochimica Acta*, vol. 437, no. 1-2, pp. 110–113, 2005.

[25] N. F. Syamimi, K. A. Matori, W. F. Lim, S. Abdul Aziz, and M. H. M. Zaid, "Effect of sintering temperature on structural and morphological properties of europium (III) oxide doped willemite," *Journal of Spectroscopy*, vol. 2014, Article ID 328931, 8 pages, 2014.

[26] D. S. Rao, P. S. Raju, B. S. Rao, and K. V. R. Murthy, "Luminescent studies of Zn_2SiO_4Mn (1.1%), Eu (1.5%) phosphor," *International Journal of Luminescence and its Application*, vol. 4, pp. 104–106, 2014.

[27] A. M. Efimov, "Section 1. Optical properties of oxide glasses; quantitative IR spectroscopy: application to studying glass structure and properties," *Journal of Non-Crystalline Solids*, vol. 203, pp. 1–11, 1996.

[28] E. M. A. Khalil, F. H. ElBatal, Y. M. Hamdy, H. M. Zidan, M. S. Aziz, and A. M. Abdelghany, "Infrared absorption spectra of transition metals-doped soda lime silica glasses," *Physica B: Condensed Matter*, vol. 405, no. 5, pp. 1294–1300, 2010.

[29] A. Dwivedi, C. Joshi, and S. B. Rai, "Effect of heat treatment on structural, thermal and optical properties of Eu^{3+} doped tellurite glass: formation of glass-ceramic and ceramics," *Optical Materials*, vol. 45, pp. 202–208, 2015.

[30] K. Omri, J. El Ghoul, A. Alyamani, C. Barthou, and L. El Mir, "Luminescence properties of green emission of SiO_2/Zn_2SiO_4:Mn nanocomposite prepared by sol-gel method," *Physica E: Low-Dimensional Systems and Nanostructures*, vol. 53, pp. 48–54, 2013.

[31] H. G. Pfeiffer and G. R. Fonda, "The zinc silicate phosphors fluorescing in the yellow and red," *Journal of the Electrochemical Society*, vol. 99, no. 4, pp. 140–143, 1952.

[32] M.-T. Tsai, Y.-F. Lu, and Y.-K. Wang, "Synthesis and characterization of manganese-doped zinc orthosilicate phosphor powders," *Journal of Alloys and Compounds*, vol. 505, no. 2, pp. 818–823, 2010.

[33] A. Manavbasi and J. C. LaCombe, "Synthesis of pure Zn_2SiO_4:Mn green phosphors by simple PVA-metal complex route," *Journal of Materials Science*, vol. 42, no. 1, pp. 252–258, 2007.